27. Yang F, Murugan R, Ramakrishna S, Wang X, Ma YX, Wang S. Fabrication of nano-structured porous PLLA scaffold intended for nerve tissue engineering. Biomaterials 2004;25:1891–1900.
28. Ghosh-Choudhury N, Windle JJ, Koop BA, Harris MA, Guerrero DL, Wozney JM, Mundy GR, Harris SE. Immortalized murine osteoblasts derived from BMP 2-T-antigen expressing transgenic mice. Endocrinology 1996;137:331–339.
29. Radin C. Random close packing of granular matter. J Stat Phys 2008;131:567–573.
30. Ehrenfried LM, Farrar D, Cameron RE. The degradation properties of co-continuous calcium phosphate polyester composites: Insights with synchrotron micro-computer tomography. J R Soc Interface 2010;7 (Suppl 5):S663–S674.
31. Lin FH, Chen TM, Lin CP, Lee CJ. The merit of sintered PDLLA/TCP composites in management of bone fracture internal fixation. Artif Organs 1999;23:186–194.
32. Ang KC, Leong KF, Chua CK, Chandrasekaran M. Compressive properties and degradability of poly(epsilon-caprolatone)/hydroxyapatite composites under accelerated hydrolytic degradation. J Biomed Mater Res A 2007;80:655–660.
33. Ehrenfried LM, Farrar D, Cameron RE. Degradation properties of co-continuous calcium-phosphate-polyester composites. Biomacromolecules 2009;10:1976–1985.
34. Wiltfang J, Merten HA, Schlegel KA, Schultze-Mosgau S, Kloss FR, Rupprecht S, Kessler P. Degradation characteristics of alpha and beta tri-calcium-phosphate (TCP) in minipigs. J Biomed Mater Res 2002;63:115–121.
35. Heidemann W, Jeschkeit S, Ruffieux K, Fischer JH, Wagner M, Kruger G, Wintermantel E, Gerlach KL. Degradation of poly(D, L)lactide implants with or without addition of calciumphosphates in vivo. Biomaterials 2001;22:2371–2381.
36. Ducheyne P, Radin S, King L. The effect of calcium phosphate ceramic composition and structure on in vitro behavior. I. Dissolution. J Biomed Mater Res 1993;27:25–34.
37. Koerten HK, van der Meulen J. Degradation of calcium phosphate ceramics. J Biomed Mater Res 1999;44:78–86.
38. Kenny SM, Buggy M. Bone cements and fillers: A review. J Mater Sci Mater Med 2003;14:923–938.
39. Leeuwenburgh SC, Wolke JG, Siebers MC, Schoonman J, Jansen JA. In vitro and in vivo reactivity of porous, electrosprayed calcium phosphate coatings. Biomaterials 2006;27:3368–3378.
40. Rush SM. Bone graft substitutes: osteobiologics. Clinics Podiatric Med Surg 2005;22:619–630.
41. Eagan MJ, McAllister DR. Biology of allograft incorporation. Clinics Sports Med 2009;28:203–214.
42. Newton CD, Nunamaker DB. Textbook of Small Animal Orthopaedics. Philadelphia. Lippincott: Lippincott; 1985.
43. Yuan H, Li Y, de Bruijn JD, de Groot K, Zhang X. Tissue responses of calcium phosphate cement: A study in dogs. Biomaterials 2000;21:1283–1290.
44. Malinin TI, Carpenter EM, Temple HT. Particulate bone allograft incorporation in regeneration of osseous defects; importance of particle sizes. Open Orthop J 2007;1:19–24.
45. Voor MJ, Arts JJ, Klein SA, Walschot LH, Verdonschot N, Buma P. Is hydroxyapatite cement an alternative for allograft bone chips in bone grafting procedures? A mechanical and histological study in a rabbit cancellous bone defect model. J Biomed Mater Res B Appl Biomater 2004;71:398–407.
46. Muzylak M, Arnett TR, Price JS, Horton MA. The in vitro effect of pH on osteoclasts and bone resorption in the cat: Implications for the pathogenesis of FORL. J Cell Physiol 2007;213:144–150.
47. Winkler T, Hoenig E, Gildenhaar R, Berger G, Fritsch D, Janssen R, Morlock MM, Schilling AF. Volumetric analysis of osteoclastic bioresorption of calcium phosphate ceramics with different solubilities. Acta Biomater 2010;6:4127–4135.

THE JOURNAL OF BONE & JOINT SURGERY

■ TRAUMA: RESEARCH

Effects of the systemic administration of alendronate on bone formation in a porous hydroxyapatite/collagen composite and resorption by osteoclasts in a bone defect model in rabbits

Y. Sugata,
S. Sotome,
M. Yuasa,
M. Hirano,
K. Shinomiya,
A. Okawa

From Tokyo Medical and Dental University, Tokyo, Japan

■ Y. Sugata, MD, Orthopaedic Surgeon, Graduate School Student
■ M. Yuasa, MD, Orthopaedic Surgeon, Graduate School Student
■ K. Shinomiya, MD, PhD, Orthopaedic Surgeon, Professor Emeritus
■ A. Okawa, MD, PhD, Orthopaedic Surgeon, Associate Professor
Department of Orthopaedic and Spinal Surgery
■ S. Sotome, MD, PhD, Orthopaedic Surgeon, Associate Professor
Development Division of Advanced Orthopaedic Therapeutics
Tokyo Medical and Dental University, 1-5-45 Yushima, Bunkyo-ku, Tokyo 113-8519, Japan.

■ M. Hirano, R & D Department Senior Manager
PENTAX New Ceramics Division, HOYA Corporation, 1-1-110 Tsutsujigaoka, Akishima-shi, Tokyo 196-0012, Japan.

Correspondence should be sent to Professor S. Sotome; e-mail: sotome.orth@tmd.ac.jp

doi:10.1302/0301-620X.93B4.25239 $2.00

J Bone Joint Surg [Br] 2011;93-B:510-16.
Received 21 May 2010; Accepted after revision 3 November 2010

Several bisphosphonates are now available for the treatment of osteoporosis. Porous hydroxyapatite/collagen (HA/Col) composite is an osteoconductive bone substitute which is resorbed by osteoclasts. The effects of the bisphosphonate alendronate on the formation of bone in porous HA/Col and its resorption by osteoclasts were evaluated using a rabbit model. Porous HA/Col cylinders measuring 6 mm in diameter and 8 mm in length, with a pore size of 100 μm to 500 μm and 95% porosity, were inserted into a defect produced in the lateral femoral condyles of 72 rabbits. The rabbits were divided into four groups based on the protocol of alendronate administration: the control group did not receive any alendronate, the pre group had alendronate treatment for three weeks prior to the implantation of the HA/Col, the post group had alendronate treatment following implantation until euthanasia, and the pre+post group had continuous alendronate treatment from three weeks prior to surgery until euthanasia. All rabbits were injected intravenously with either saline or alendronate (7.5 μg/kg) once a week. Each group had 18 rabbits, six in each group being killed at three, six and 12 weeks post-operatively. Alendronate administration suppressed the resorption of the implants. Additionally, the mineral densities of newly formed bone in the alendronate-treated groups were lower than those in the control group at 12 weeks post-operatively. Interestingly, the number of osteoclasts attached to the implant correlated with the extent of bone formation at three weeks.

In conclusion, the systemic administration of alendronate in our rabbit model at a dose-for-weight equivalent to the clinical dose used in the treatment of osteoporosis in Japan affected the mineral density and remodelling of bone tissue in implanted porous HA/Col composites.

A wide variety of bone substitutes have been developed that include sintered calcium phosphates and their composites, with their clinical use having increased over the past decade.[1] Recently, other types of bone substitutes have also been developed, including a hydroxyapatite/collagen (HA/Col) composite.[2,3] In contrast to sintered hydroxyapatite (HA), which is barely resorbed after implantation, HA/Col is resorbed by osteoclast-like cells and is involved in natural remodelling of bone. The coupling mechanisms between osteoblasts and osteoclast -like cells are thought to contribute to this material's osteoconductibility. The porous nature of HA/Col has a sponge-like elasticity and affords excellent biocompatibility and osteoconductibility.[4,5] It has a large surface area of 75 m^2/g owing to its composition of 80% nanoscale HA crystals enabling it to adsorb a large quantity of proteins, such as growth factors, and other molecules, as well as drugs and ions.[3,6]

Bisphosphonates are synthetic analogues of pyrophosphate, and were first synthesised in 1865 and used in industry as a corrosion inhibitor.[7,8] Etidronate was the first bisphosphonate to be used clinically in the treatment of myositis ossificans.[7] In 1976, the effectiveness of etidronate for the treatment of osteoporosis was reported, although the biological mechanisms had not been clarified.[9] Subsequently, the mechanism of action of bisphosphonate was established, permitting the development of other bisphosphonates,

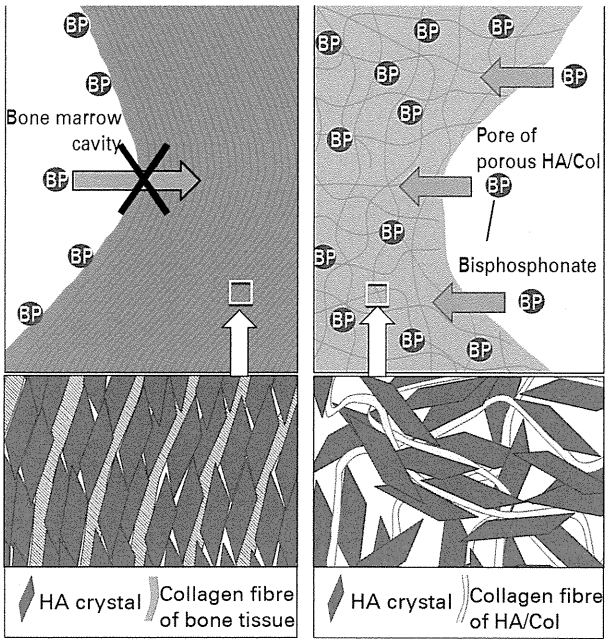

Fig. 1

Diagrams showing the adsorption of bisphosphonates (BP) onto the hydroxyapatite (HA) at the surface only of bone tissue (left panel), but adsorption into the numerous pores within the hydroxyapatite/collagen (HA/Col) composite (right panel).

including alendronate, which is more effective than first-generation bisphosphonates in the treatment of osteoporosis. Bisphosphonates have a high affinity for HA and are adsorbed onto the HA contained in bone after they are administered. When osteoclasts dissolve HA and resorb bone, bisphosphonates are released and taken up by the osteoclasts to initiate apoptosis, thereby leading to decreased bone resorption.[10-14]

Administered bisphosphonates are also adsorbed onto the HA surfaces of implanted porous HA/Col. Whereas the HA nanocrystals contained in natural bone are bound to each other so compactly that bisphosponates adsorb only onto HA at the surface of the bone,[15,16] the HA nanocrystals in HA/Col are not bound to each other as tightly. This permits bisphosphonates to penetrate into the material through the numerous pores in the HA/Col (Fig. 1). Given this, we suspect that bisphosphonates will influence the bone formation and resorption of implanted porous HA/Col, although whether they affect fracture healing is still controversial.[17,18]

There have been few reports about the effects of bisphosphonates on the healing process and on the resorption of bioabsorbable bone substitutes,[19] although there are some reports about their effects on allograft[20-23] and autograft bone.[24-26] In this study, we transplanted porous HA/Col into bone defects of rabbit femora and evaluated the effects of alendronate (ALN) on bone formation and on the resorption of HA/Col by osteoclasts.

Materials and Methods

HA/Col nanocomposite fibres were synthesised from atelocollagen derived from porcine skin, $Ca(OH)_2$, and H_3PO_4 using a co-precipitation method described previously.[2] In brief, atelocollagen (Nitta Gelatin Co., Osaka, Japan) was dissolved in an H_3PO_4 solution. Both the dissolved collagen and a $Ca(OH)_2$ suspension were added to distilled water and placed in a water bath that was thermally stabilised at 40°C. The speed of each addition was controlled to maintain the pH at 9.0. The initial materials were measured so that the final HA/Col nanocomposites would have an 80:20 weight-to-ratio composition. The HA/Col fibres were lyophilised to prepare porous HA/Col implants. Porous HA/Col implants were produced by homogenising the HA/Col fibres (1 g) with 6.5 ml of phosphate-buffered saline and alkalising with 50 µl of a 1 M sodium hydroxyapatite solution. The resultant solution was mixed with 1.5 ml of a 0.6% collagen solution dissolved in phosphoric acid (pH 2.0). The mixture, now at pH 7.0, was infused into a mould. In order to initiate the gelation of the collagen as a binder, the mould containing the mixture was incubated at 37°C for two hours. The HA/Col gel produced was frozen at -60°C, and the liquid within the mixture formed ice crystals in the gel. The spaces occupied by the ice crystals were converted into pores by subsequent lyophilisation. The lyophilised porous HA/Col constructs were cross-linked by thermal dehydration at 140°C under vacuum, cut into cylindrical shapes 6 mm in diameter and 8 mm long, and sterilised by irradiation (Fig. 2). The porosity of the implants was 95%, as calculated from the compositional ratio of the HA/Col fibres and water. The pore size ranged from 100 µm to 500 µm and was measured using the intercept method. Owing to the preparation method for the ice crystals, there was some unevenness in the distribution of pore sizes and shapes among the implants, which could not be evaluated quantitatively.

Surgical procedure. The experiment was conducted using 72 three-month-old male Japanese white rabbits. Their mean weight was 3.15 kg (2.8 to 3.3) (CLEA Japan Inc., Tokyo, Japan), and the study was approved by the Animal Committee of Tokyo Medical and Dental University. The rabbits were anaesthetised by an intramuscular injection of medetomidine sodium (Domitor, 0.5 ml/kg; Nippon Zenyaku Kogyo Co. Ltd, Fukushima, Japan) and ketamine hydrochloride (Ketalar, 0.5 ml/kg; Daiichi Sankyo Co. Ltd, Tokyo, Japan). Under sterile conditions, an incision was made in the lateral aspect of the right distal femur. The periosteum was detached and a full-thickness unicortical and trabecular bone resection was performed on the lateral condyle using a 5 mm diameter trephine drill with continuous saline irrigation to prevent thermal necrosis of the margins. After the drilling, the debris and remnants of the bone marrow were removed by flushing the area with saline, and the implants were inserted into the bone bed that had been created.

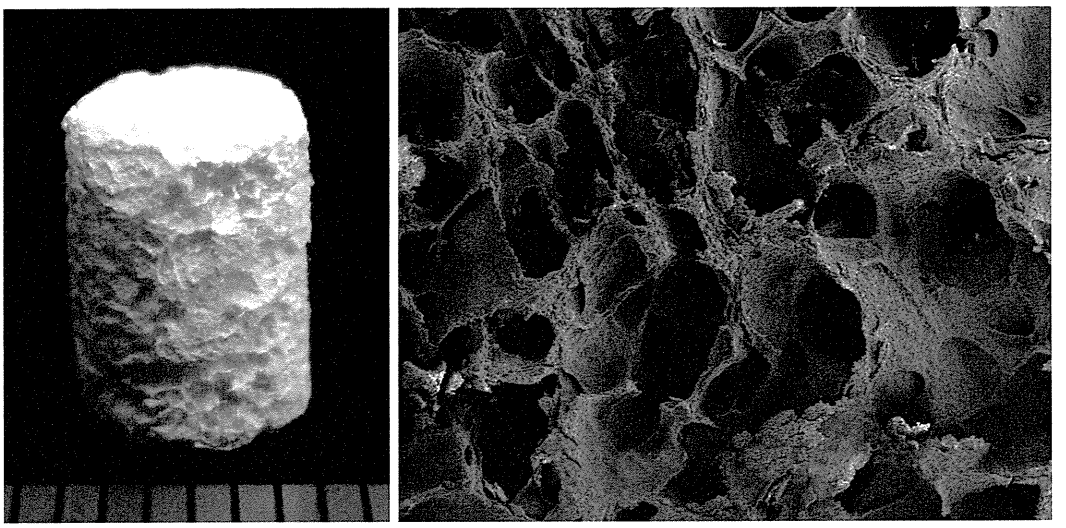

Fig. 2

Photograph (left) and scanning electron microscopy image (right, magnification × 20) showing the porous hydroxyapatite/collagen compound prepared as a cylinder 6 mm in diameter and 8 mm in length. The pore sizes ranged from 100 μm to 500 μm.

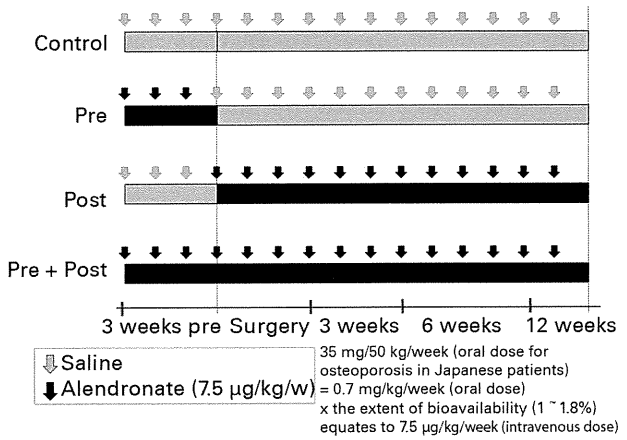

Fig. 3

Diagram showing the injection protocol. Rabbits were divided into four groups: a saline control group (control), a systemic alendronate pre-administration group (pre), a post-administration group (post), and a pre-post continuous group (pre+post). All rabbits received saline or 7.5 μg/kg alendronate intravenously each week. The dose was calculated to correspond with alendronate administration in humans with osteoporosis in Japan.

Injection protocol. The total experimental period was 15 weeks and consisted of a three-week ALN pre-treatment period and a 12-week post-operative observation period. The rabbits were divided randomly into four groups (n = 18), a control group and three systemic alendronate sodium hydrate (ALN; Teijin Pharma Ltd, Tokyo, Japan) administration groups. The three active groups were the 'pre' group, which received ALN pre-treatment for three weeks before surgery, the 'post' group, which received ALN treatment beginning post-operatively until euthanasia, and the pre+post group, which received continuous ALN treatment from three weeks before surgery until euthanasia. All rabbits received either 0.9% saline or ALN (7.5 μg/kg) intravenously once a week throughout the experimental period (Fig. 3). The dose of alendronate was adjusted according to the usual dose for the treatment of osteoporosis in Japan (35 mg/week) and the extent of bioavailability.[27] A total of six rabbits from each group were killed at three, six and 12 weeks post-operatively, and the right distal femora were collected and cleansed of soft tissues. These bone specimens were fixed in 4% paraformaldehyde and 0.025% glutaraldehyde for one week at 4°C.

Three-dimensional micro-CT analysis of bone. Imaging of the femora was performed using a micro-CT apparatus (Scan Xmate-E090; Comscan Techno Co., Kanagawa, Japan), and three-dimensional (3D) micro-CT images were analysed using image analysis software (TRI/3D-BON; Ratoc System Engineering Co., Tokyo, Japan). The mineral density of the extracted bone tissue and the region of implantation were calculated. Briefly, the evaluation zone was defined as the implanted cylindrical site without a cortical aperture, of which both the diameter and the length were 6 mm. The mineral density of each voxel in the area (Fig. 4) was calculated from the CT Hounsfield number using a standard curve. Before analysis, the mineral densities of porous HA/Col pieces, excluding the pores, were found to be uniformly 220 mg/cm^3. Accordingly, in order to identify which voxels represented bone tissue, a mineral density threshold was set at 400 mg/cm^3, and the area above the threshold was defined as bone tissue (Fig. 4).

Histological examination. The dissected distal femora were decalcified in 20% ethylenediaminetetra-acetic acid, dehydrated with a gradient ethanol series, and embedded in

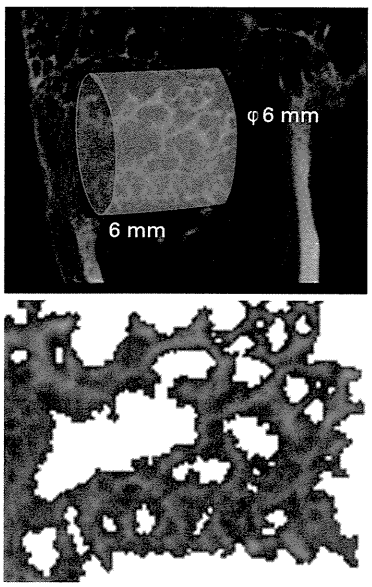

Fig. 4

Micro-CT scan showing the harvested bone tissue (upper panel) and a diagram showing extracted bone tissue with a mineral density > 400 mg/cm^3 (lower panel). (ϕ, diameter).

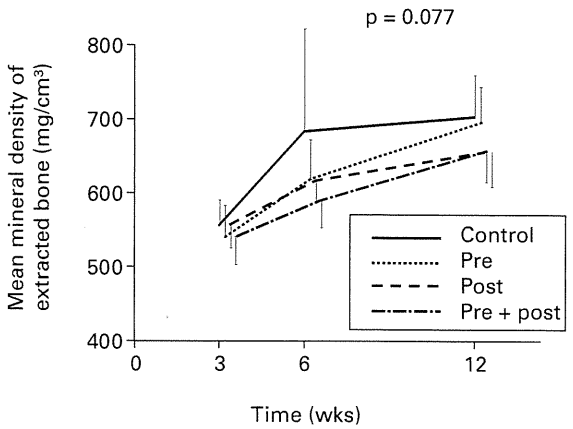

Fig. 5

Graph showing the mean mineral density of the extracted bone in each group and at each study period. The error bars show SD.

paraffin. Based on macroscopic observation, coronal sections 5 μm thick, including the centre of the implant area, were prepared. Haematoxylin and eosin (H&E) staining was used to quantify the residual HA/Col area and the bone-tissue area; tartrate-resistant acid phosphatase (TRAP) staining was used to quantify the number of osteoclasts present. The border between the residual HA/Col and the surrounding bone tissue was clearly recognised because residual HA/Col was easily identified by its distinctive layer structure and staining intensity which is lower than bone in H&E-stained sections. The residual HA/Col area, bone-tissue area and TRAP-positive cell number were measured using ImageJ software (NIH, Bethesda, Maryland).

Statistical analysis. In each experiment, the overall differences between groups were determined by two-factor analysis of variance (ANOVA), and Pearson's product-moment correlation coefficient (r) was used to study the relationship between the number of osteoclasts and the area of bone formation. Statistical significance was set at $p < 0.05$.

Results

Micro-CT analysis. Tissue from the cylindrical implant area with mineral density > 400 mg/cm^3 was identified as bone and was used for the analysis. The mineral densities of the extracted material, which are thought to correlate with the maturity and quality of the bone formed, are shown in Figure 5. Although the overall differences between the groups were not significant (ANOVA, $p = 0.077$), the mean density of the control group tended to be higher than that of the other groups at six weeks; however, there was considerable variability in the individual samples. In addition, the mean densities of the control and pre groups also tended to be higher than those of the post and pre+post groups at 12 weeks. The total mineral content, defined as the product of the mineral density and bone volume, was also calculated. There were no significant differences between the groups, and the content values were highly variable ($p = 0.268$).

Histological evaluation. Figure 6 shows representative H&E-stained coronal sections. At three weeks after surgery, the implant structures in every group were generally still well-defined shapes, containing inconsistent pore shapes. Active bone formation and formed bone were observed adjacent to the implants and inside the pores, although there were individual differences, which might be due to the irregular surfaces of the implants rather than to differences between the groups. At six weeks the areas of the implants in each group were reduced, as also was the area of the formed bone, especially in the ALN-treated groups, compared with the results at three weeks. In particular, in the post and pre+post groups, the exposed remnants of the implant without surrounding bone tissue were more numerous. At 12 weeks, the residual HA/Col became smaller and more scattered in the implant areas. In the control group most of the remnants were surrounded by formed bone and active osteoblasts were still attached to some of the surrounding bone. In the post and pre+post groups, not only were the residual implants larger than in the control group, but the amounts of remnants exposed directly to bone marrow without surrounding bone tissue were larger than that in the control group (Fig. 6).

Quantitative evaluation of histological findings. In a coronal section at the centre of the implant, the areas of residual HA/Col (Fig. 7) and the areas of bone tissue in the bone marrow cavity were measured. The areas of HA/Col decreased over time, especially after six weeks. Although the overall differences between the groups were not significant (ANOVA, $p = 0.115$), the residual HA/Col area of the

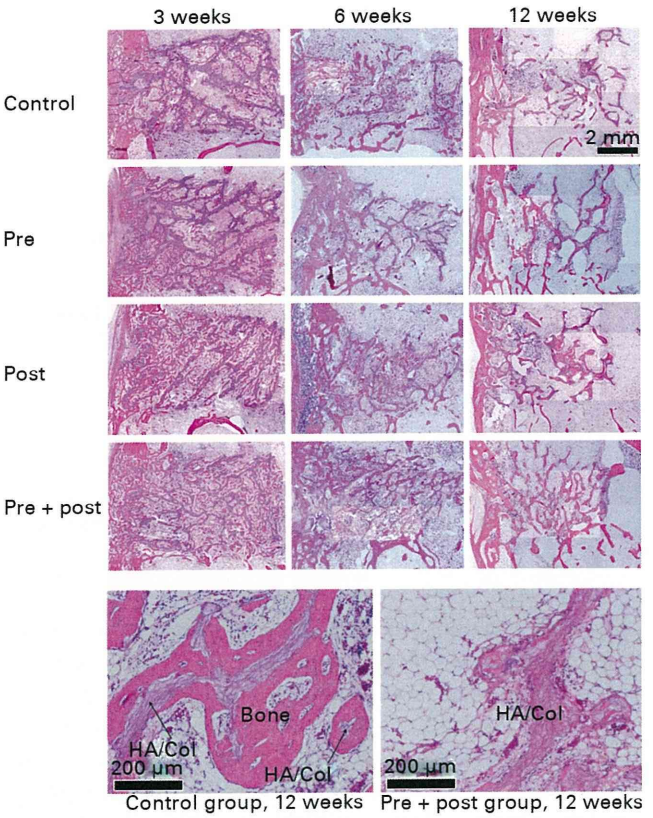

Fig. 6

Photomicrographs of representative coronal sections at the centre of the implants (haematoxylin & eosin-stained). At 12 weeks, the hydroxyapatite/collagen (HA/Col) in the control group was almost resorbed and was surrounded by bone, whereas large portions of HA/Col without bone were frequently observed in the groups that received alendronate for any duration.

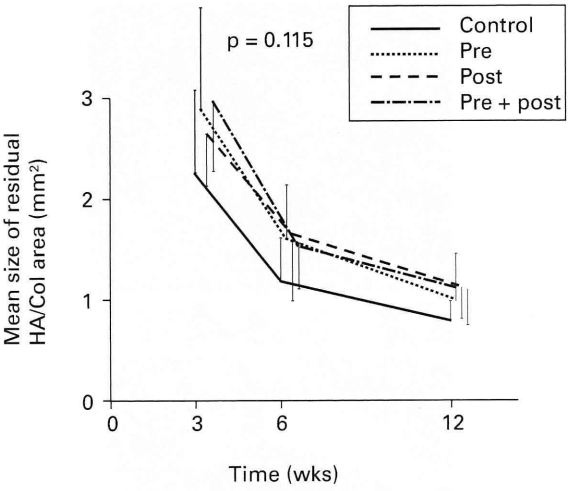

Fig. 7

Graph showing the mean residual area of hydroxyapatite/collagen (HA/Col) at each time interval and in each group. The error bars show SD.

control group tended to be lower throughout the experimental period than in the other groups, in which the HA/Col areas were almost equivalent at every time point. The measurement of the bone-tissue area varied widely in each sample, as shown in the micro-CT analysis of the total mineral content.

In TRAP-stained sections, there were large numbers of TRAP-positive osteoclasts (Fig. 8a). Most of the TRAP-positive cells were not attached to bone but instead to the implant throughout the experimental period, but the number of cells varied widely in each section. Figure 8b shows the ratio of the mean number of osteoclasts attached directly to the HA/Col material to the total length of the edge of the implant. At six weeks, despite the increased ratio in the control group, the continuously ALN-treated groups did not show increases in this ratio. However, the overall difference between the groups was not statistically significant (ANOVA, $p = 0.184$) and the ratios varied extensively, especially in the control group and the ALN pre-treatment group. Correlations between the bone area and number of osteoclasts at three weeks, regardless of the group, are shown in Figure 8c. A relatively high statistically positive correlation was observed ($r = 0.691$).

Discussion

We evaluated the effect of ALN on bone formation in the presence of a porous HA/Col implant. The amount of ALN administered to the rats in this study was chosen to represent the dose for weight equivalent for patients being treated for osteoporosis in Japan (35 mg/week).[27] This dose was selected to allow extrapolation of the effects of the clinical use of bisphosphonate after the implantation of bone substitutes. It should be noted that in most other countries doses twice as large (70 mg/week) are used.

The mineral densities in the post and pre+post groups tended to be lower than those of the control and pre group at 12 weeks. Bisphosphonates are synthetic analogues of pyrophosphate, which has an affinity for HA and inhibits mineralisation.[28] Therefore, first-generation bisphosphonates strongly inhibit mineralisation and have been used as anti-calcification agents.[29] ALN is a second-generation bisphosphonate which has little anti-calcification effect at the dose used to treat osteoporosis, but at much higher doses does exert an anti-calcification action. However, in this study, the dose of ALN reduced the mineral density of the bone tissue formed at the implant site. The porous HA/Col of the ALN-treated groups were thought to contain ALN at high densities, and the drilling of a hole and the implantation of HA/Col induced a higher bone turnover as a reaction to the implantation itself. In general, bisphosphonates tend to deposit bone tissue with vigorous bone turnover. These facts suggest the possibility that local redistribution of the ALN occurs as a result of the HA/Col being resorbed by osteoclasts to the newly formed bone, producing a higher concentration of ALN than appropriate for the treatment of osteoporosis. As a result, not only would the osteoclast activity and related osteoblast activity be inhibited by the ALN in the implant, but the ALN

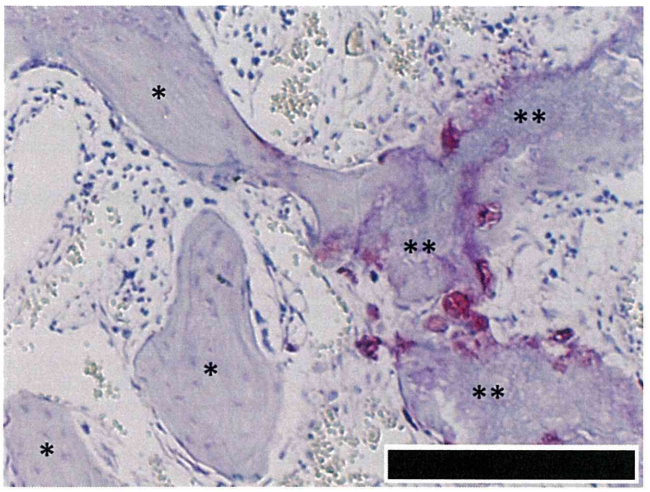

Fig. 8a

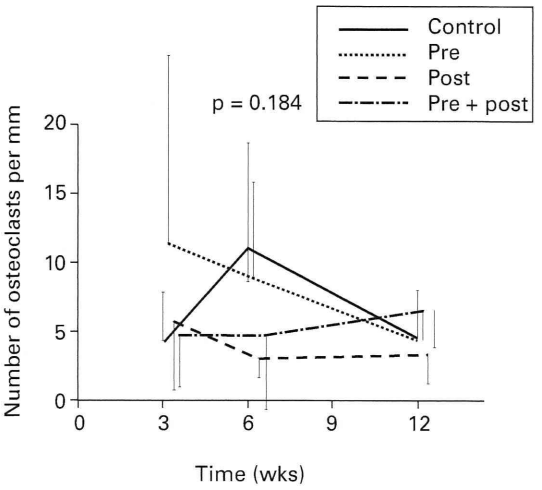

Fig. 8b

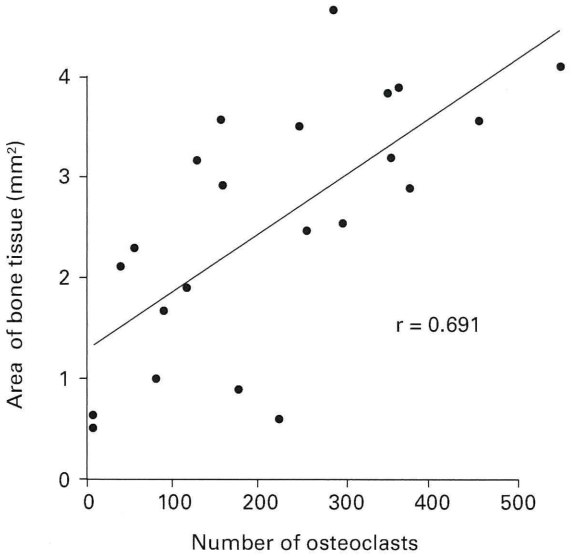

Fig. 8c

Figure 8a – photomicrograph showing most of the tartrate-resistant acid phosphatase (TRAP)-positive cells are attached to the remnant of the implant (TRAP staining). *, bone; **, residual hydroxyapatite/collagen (HA/Col). The scale bar is 200 μm. Figure 8b – graph showing the ratio of the number of osteoclasts attached to the HA/Col to the total length of the implant, in each group and at each time interval.The error bars show SD. Figure 8c – scatter plot of the area of bone tissue *versus* the number of osteoclasts, regardless of the group, with a line of best fit (correlation coefficient r = 0.691).

accumulating in the new bone would prevent mineralisation, and thereby the mineral density might be reduced.

The quantitative analysis of the HA/Col remnant revealed an inhibitory effect of ALN on osteoclast-induced resorption of HA/Col. Analysis of the ratio of osteoclast numbers to the length of the HA/Col surface showed no increase at six weeks after surgery in the continuously ALN-treated groups, although the control and pre groups showed relatively high ratios. These results suggest that systemically administered ALN inhibits osteoclast activity and resorption of the transplanted HA/Col.

At three weeks, most of the osteoclasts at the transplanted site were attached to the HA/Col and actively resorbing it. In contrast to the HA/Col resorption, the number of osteoclasts attached to the bone tissue of the transplanted site was very small, and the bone tissue resorption by the osteoclasts was negligible at three weeks postoperatively. Therefore, the bone volume at the transplanted site at three weeks is thought to be an indicator of the bone formation activity of the osteoblasts, and the strong correlation between the number of osteoclasts attached to HA/Col and the area of bone-tissue suggests coupling

mechanisms between osteoblasts and the osteoclasts that resorb HA/Col. HA in the bone tissue has an affinity for a wide variety of molecules, including growth factors, which can affect bone remodelling. Therefore, the following mechanism is thought to be involved in bone remodelling. HA is a reservoir of growth factors, which are released when the HA is resorbed by osteoclasts, thereby affecting bone remodelling. The importance of this mechanism in natural bone has recently been questioned.[30] The HA in porous HA/Col also has the same affinity for such molecules, and the adsorptive area of HA/Col is larger than that of natural bone, as stated above. Therefore, this osteoclast-osteoblast coupling mechanism might not be negligible at HA/Col transplanted sites.

In conclusion, our data suggest that the systemic administration of ALN affects the mineral density and remodelling of bone tissue formed at the implant site of HA/Col, although a statistically significant difference was not demonstrated in our model when using a dose representing the dose used in the treatment of osteoporosis in Japan. This study suggests that it might be beneficial to suspend the administration of bisphosphonates after the implantation of HA/Col or other bioabsorbable bone substitutes, at least until the implants are resorbed, although further studies are needed to understand this process better.

Porous HA/Col was jointly developed by the Tokyo Medical and Dental University, the HOYA Corporation (Tokyo, Japan), and the National Institute for Materials Science (NIMS). We thank Dr M. Kikuchi at NIMS for his technical support and advice. This work was supported by a Grant-in-Aid for Scientific Research from the Ministry of Education, Culture, Sports, Science, and Technology of Japan.

No benefits in any form have been received or will be received from a commercial party related directly or indirectly to the subject of this article.

References

1. **Urabe K, Itoman M, Toyama Y, et al.** Current trends in bone grafting and the issue of banked bone allografts based on the fourth nationwide survey of bone grafting status from 2000 to 2004. *J Orthop Sci* 2007;12:520-5.
2. **Kikuchi M, Itoh S, Ichinose S, Shinomiya K, Tanaka J.** Self-organization mechanism in a bone-like hydroxyapatite/collagen nanocomposite synthesized in vitro and its biological reaction in vivo. *Biomaterials* 2001;22:1705-11.
3. **Itoh S, Kukuchi M, Takakuda K, et al.** Implantation study of a novel hydroxyapatite/collagen (HAp/col) composite into weight-bearing sites of dogs. *J Biomed Mater Res* 2002;63:507-15.
4. **Tsuchiya A, Sotome S, Asou Y, et al.** Effects of pore size and implant volume of porous hydroxyapatite-collagen (HAp/Col) on bone formation in a rabbit bone defect model. *J Med Dent Sci* 2008;55:91-9.
5. **Kawasaki Y, Sotome S, Yoshii T, et al.** Effects of gamma-ray irradiation on mechanical properties, osteoconductivity, and adsorption of porous hydroxyapatite/collagen. *J Biomed Mater Res B Appl Biomater* 2010;92:161-7.
6. **Sotome S, Uemura T, Kikuchi M, et al.** In vitro evaluation of highly absorptive ceramics materials needs consideration of calcium and magnesium ions adsorbed to the materials. *Key Engineering Materials* 2002;218:153-6.
7. **Fleisch H.** Bisphosphonates: mechanisms of action. *Endocr Rev* 1998;19:80-100.
8. **Fleisch H.** Development of bisphosphonates. *Breast Cancer Res* 2002;4:30-4.
9. **Heaney RP, Saville PD.** Etidronate disodium in postmenopausal osteoporosis. *Clin Pharmacol Ther* 1976;20:593-604.
10. **Russell RGG, Watts NB, Ebetino FH, Rogers MJ.** Mechanisms of action of bisphosphonates: similarities and differences and their potential influence on clinical efficacy. *Osteoporos Int* 2008;19:733-59.
11. **Benford HL, McGowan NW, Helfrich MH, Nuttall ME, Rogers MJ.** Visualization of bisphosphonate-induced caspase-3 activity in apoptotic osteoclasts in vitro. *Bone* 2001;28:465-73.
12. **Fisher JF, Rogers MJ, Halasy JM, et al.** Alendronate mechanism of action: geranylgeraniol, an intermediate in the mevalonate pathway, prevents inhibition of osteoclast formation, bone resorption, and kinase activation in vitro. *Proc Natl Acad Sci U S A* 1999;96:133-8.
13. **van beek E, Löwik C, van de Pluijm G, Papapoulos S.** The role of geranylgeranylation in bone resorption and its suppression by bisphosphonates in fetal bone explants in vitro: a clue to the mechanism of action of nitrogen-containing bisphosphonates. *J Bone Miner Res* 1999;14:722-9.
14. **Luckman S, Hughes D, Coxon F, et al.** Nitrogen-containing bisphosphonates inhibit the mevalonate pathway and prevent post-translational prenylation of GTP-binding proteins, including Ras. *J Bone Miner Res* 1998;13:581-9.
15. **Azuma Y, Sato H, Oue Y, et al.** Alendronate distributed on bone surfaces inhibits osteoclastic bone resorption in vitro and in experimental hypercalcaemia models. *Bone* 1995;16:235-45.
16. **Sato M, Grasser W, Endo N, et al.** Bisphosphonate action: alendronate localization in rat bone and effects on osteoclast ultrastructure. *J Clin Invest* 1991;88:2095-105.
17. **Li , Mori S, Li J, et al.** Long-term effect of incadronate disodium (YM-175) on fracture healing of femoral shaft in growing rats. *J Bone Miner Res* 2001;16:429-36.
18. **Amanat N, Brown R, Bilston L, Little D.** A single systemic dose of pamidronate improves bone mineral content and accelerates restoration of strength in a rat model of fracture repair. *J Orthop Res* 2005;23:1029-34.
19. **Spence G, Phillips S, Campion C, Brooks R, Rushton N.** Bone formation in a carbonate-substituted hydroxyapatite implant is inhibited by zoledronate: the importance of bioresorption to osteoconduction. *J Bone Joint Surg [Br]* 2008;90-B:1635-40.
20. **Aspenberg P, Astrand J.** Bone allografts pretreated with a bisphosphonate are not resorbed. *Acta Orthop Scand* 2002;73:20-3.
21. **DiResta G, Manoso M, Naqvi A, et al.** Bisphosphonate delivery to tubular bone allografts. *Clin Orthop* 2008;466:1871-9.
22. **Jakobsen T, Baas J, Bechtold J, Elmengaard B, Søballe K.** The effect of soaking allograft in bisphosphonate: a pilot dose-response study. *Clin Orthop* 2010;468:867-74.
23. **Agholme F, Aspenberg P.** Experimental results of combining bisphosphonates with allograft in a rat model. *J Bone Joint Surg [Br]* 2009;91-B:670-5.
24. **Takahata M, Ito M, Abe Y, Abumi K, Minami A.** The effect of anti-resorptive therapies on bone graft healing in an overiectomized rat spinal arthrodesis model. *Bone* 2008;43:1057-66.
25. **Huang R, Khan S, Sandhu H, et al.** Alendronate inhibits spine fusion in a rat model. *Spine* 2005;30:2516-22.
26. **Xue Q, Li H, Zou X, et al.** The influence of alendronate treatment and bone graft volume on posterior lateral spine fusion in a porcine model. *Spine* 2005;30:1116-21.
27. **Lin J, Duggan D, Chen I, Ellsworth R.** Physiological disposition of alendronate, a potent anti-osteolytic bisphosphonate, in laboratory animals. *Drug Metab Dispos* 1991;19:926-32.
28. **Thouverey C, Bechkoff G, Pikula S, Buchet R.** Inorganic pyrophosphate as a regulator of hydroxyapatite or calcium pyrophosphate dihydrate mineral deposition by matrix vesicles. *Osteoarthritis Cartilage* 2009;17:64-72.
29. **Nollen A.** Effects of ethylhydroxydiphosphonate (EHDP) on heterotopic ossification. *Acta Orthop Scand* 1986;57:358-61.
30. **Matsuo K, Irie N.** Osteoclast-osteoblast communication. *Arch Biochem Biophys* 2008;473:201-9.

Original Contribution

Kurume Medical Journal, 57, 101-108, 2010

"Hybrid Exercise" Prevents Muscle Atrophy in Association with a Distinct Gene Expression Pattern

TORU MATSUGAKI*, NAOTO SHIBA*,**, SHOHEI KOHNO†, TAKESHI NIKAWA†, KATSUYA HIRASAKA†, YUUSHI OKUMURA†, KAZUMI ISHIDOH‡, TAKASHI SOEJIMA*, KAZUHIRO YOSHIMITSU* AND KENSEI NAGATA*

**Department of Orthopedics, Kurume University School of Medicine, Kurume 830-0011,*
***Rehabilitation Center, Kurume University Medical Center, Kurume 839-0863,*
†Department of Nutritional Physiology, Institute of Health Biosciences, The University of Tokushima Graduate School, Tokushima 770-8503 and
‡Institute for Health Sciences, Tokushima-Bunri University, Tokushima 770-8514, Japan

Received 27 August 2010, accepted 4 October 2010

Edited by KOJI TOYOMASU

Summary: "Hybrid exercise" utilizing combined electrical stimulation and voluntary muscle contraction has been developed as a muscle exercise method. Although our previous studies have confirmed the effectiveness of the procedure, the mechanisms of its efficacy still remain unclear. In the present study, we identified genes that are specifically expressed in disused muscles, using the semitendinosus muscle from patients who underwent anterior cruciate ligament (ACL) reconstruction. Preoperative exercise was performed by four ACL-injured patients, who were subjected either to hybrid exercise (n=2), electrical stimulation (n=1), or no electrical stimulation (n=1), in addition to standard weight training for 4 weeks. Cross-sectional area (CSA) of the semitendinosus muscle was measured before and after the exercise by magnetic resonance imaging (MRI). A piece of the semitendinosus muscle was isolated during the surgery, and comprehensive analysis of the gene expression in this sample was performed using DNA microarray analysis. CSA increased in size by 4.2 and 14.7%, respectively, after hybrid exercise, and by 1.4% after electrical stimulation. However it shrunk by 7.7% without electrical stimulation. DNA microarray analysis revealed that hybrid exercise was more effective at stimulating the expression of signal transduction-, transcription- and cytoskeleton-related genes in semitendinosus muscles than electrical stimulation alone. In particular, gene ontology analysis revealed that hybrid exercise induced significantly higher expression of eukaryotic translation initiation factor 5A (EIFSA), peroxisomal biogenesis factor 6 (PEX6) and histone cluster 1 H4 (HIST1H4), compared with electrical stimulation alone. The expression of signal transduction-, transcription- and cytoskeleton-related genes may play an important role in muscle bulk increasing mechanisms in hybrid exercise.

Key words anterior cruciate ligament-injured patients, neuromuscular electrical stimulation, gene expression, muscle strengthening exercise, disuse-induced muscle atrophy

Corresponding author: Naoto Shiba, M.D. and Ph.D., Department of Orthopedics, Kurume University School of Medicine, 67 Asahi-machi, Kurume 830-0011, Japan. Tel: 0942-31-7568 Fax: 0942-35-0709 E-mail: nshiba@med.kurume-u.ac.jp

Abbreviations: ACL, anterior cruciate ligament; AM, adductor muscles; BFL, biceps femoris long head; BFS, biceps femoris short head; CSA, cross-sectional area; EIF5A, eukaryotic translation initiation factor 5A; FHOD3, formin homology 2 domain containing 3; GAPDH, glyceraldehyde-3-phosphate dehydrogenase; GM, gracilis muscle; GO, gene ontology; HIST1H4, histone cluster 1 H4; MRI, magnetic resonance imaging; PEX6, peroxisomal biogenesis factor 6; RF, rectus femoris; RT-PCR, reverse transcription and polymerase chain reaction; SaM, sartorius muscle; SM, semimembranosus muscle; ST, semitendinous muscle; VI, vastus intermedius; VL, vastus lateralis; VM, vastus medialis.

INTRODUCTION

We recently developed a "hybrid exercise" technique that resists the motion of a volitionally contracting muscle by means of a force generated by an electrically stimulated antagonist (Fig. 1) [1-4]. This technique utilizes electrically stimulated eccentric contractions and concentric volitional contractions involving reciprocal limb movements, and requires minimal external stabilization as compared with conventional weight training. Matsuse et al. [1] have shown that such hybrid exercise increased the extension torque of the elbow joint by about 30% and the cross-sectional areas (CSA) of the proximal upper extremity muscles by about 15% over a 12-week period. In addition, Iwasaki et al. [2] demonstrated that 6 weeks of hybrid exercise effectively increased the extension torque of the knee joint by 19-33%. Takano et al. also demonstrated that 12 weeks of hybrid exercise increased the knee extension torque by 39% and the CSA of quadriceps muscle by 9% in elderly subjects [3]. However, the mechanism by which hybrid exercise achieves these increases in muscular strength and bulk are still unknown.

Muscle atrophy occurs as a consequence of denervation, injury, joint immobilization, bed rest, glucocorticoid treatment, sepsis, cancer, and aging [5]. Unfortunately, there is no effective treatment for muscle atrophy. The maintenance of muscle mass is controlled by a balance between protein synthesis and protein degradation pathways, which is thought to shift toward protein degradation during atrophy [5]. Recently, a signaling pathway that increases protein synthesis was shown to promote muscle hypertrophy, thereby overcoming muscle atrophy [6,7]. This finding led us to examine the effects of hybrid exercise on muscle power and muscle bulk in disuse-induced atrophic muscle at the genetic level. In the present study, we examined the gene expression profile in atrophied muscles of patients who underwent hybrid exercise.

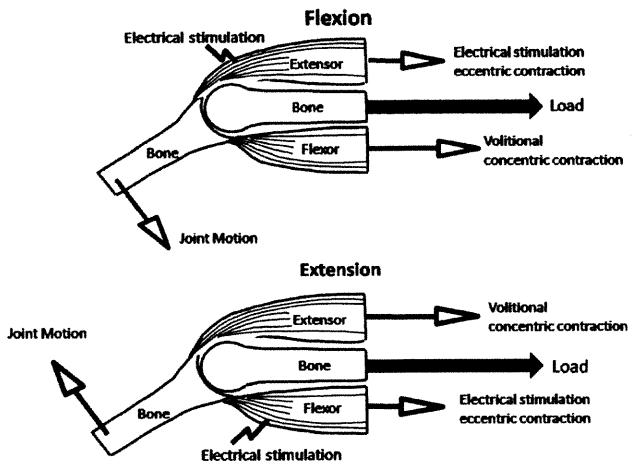

Fig. 1. Schematic model of hybrid exercise.
Hybrid exercise resists utilizes electrically stimulated eccentric contractions and concentric volitional contractions with reciprocal limb movements. Both the volitionally activated agonist and the electrically stimulated antagonist contract during joint motion. The result is that both muscles are trained and that a longitudinal compressive load is placed on the bone.

MATERIALS AND METHODS

Subjects and exercise procedure

Four patients with anterior cruciate ligament (ACL) injuries were recruited for this study. Their average age was 17.8 years old (range 15-24). They were all scheduled to undergo ACL reconstruction surgery, and were subjected either to hybrid exercise (n=2), electrical stimulation (control 1; n=1) or no electrical stimulation (control 2; n=1), as described below. The subjects exercised three times a week for four weeks immediately before the ACL reconstruction surgery, and the exercises were done only on the affected side. Patients in all three groups were routinely subjected to half squat and calf raise exercise as standard weight training. One section of the standard weight training consisted of 5 sets of 20 repetitions.

All protocols used in this study were approved by the Ethics Committee of Kurume University (approved NO.06009). Following approval, informed consent was obtained from the subjects who had reviewed the goals of the study and agreed to participate. For minor subjects, approval was also obtained from their legal guardian.

Hybrid exercise

The subjects in this group were made to sit in a chair. The hamstring muscle was then electrically stimulated during volitional knee extension, and the quadriceps muscle was stimulated during volitional knee flexion. Each session included 10 sets of 10 reciprocal 3-sec (30°/sec) knee extensions and flexions. The sets were separated by 1-min rest intervals, and an exercise session required 19 min to complete. The electrical stimulation device has been described previously [8]. The stimulation waveform used in this study was similar in some ways to that used in "Russian stimulation [9]," and consisted of a 5,000 Hz carrier frequency modulated at 20 Hz (2.4 ms on, 47.6 ms off) to deliver

a rectangular biphasic pulse [3,8]. The stimulation intensities were set at 70% of the maximum comfortable intensity, which was determined by increasing the stimulation voltage until the subjects reported any discomfort, for the quadriceps muscle, and at 80% of that for the hamstring muscle [3].

Electrical stimulation

The subject was instructed to relax and not to attempt a volitional muscle contraction with the knee immobilized in a brace at full extension. The wave form, frequency, stimulation intensity and number of repetitions were the same as for the subject receiving hybrid exercise.

Measurement of cross-sectional areas of semitendinosus muscles

CSA of the semitendinosus muscle which would be collected for subsequent DNA microarray analyses was measured by means of magnetic resonance imaging: MRI (Signa LX 1.5 Tesla; GE Healthcare, New York, NY, USA) (Fig. 2). Consecutive transaxial T1-weighted images (spin-echo; TR=720 ms, TE=0.7 ms, matrix size=384×256, FOV=48 cm×36 cm, slice thickness=8 mm, inter slice gap=2 mm) were obtained. The subjects were scanned in a supine position with the knee fully extended and the ankles fixed by an apparatus which was designed especially for this study. The number of transaxial images obtained for each subject was 30. From these images, the image that corresponded to the middle region along the length of the thigh was chosen. CSAs of the semitendinosus muscle were all analyzed by a blinded assessor using NIH Image software (Image J, version 1.410; NIH, Bethesda, MD, USA) [3].

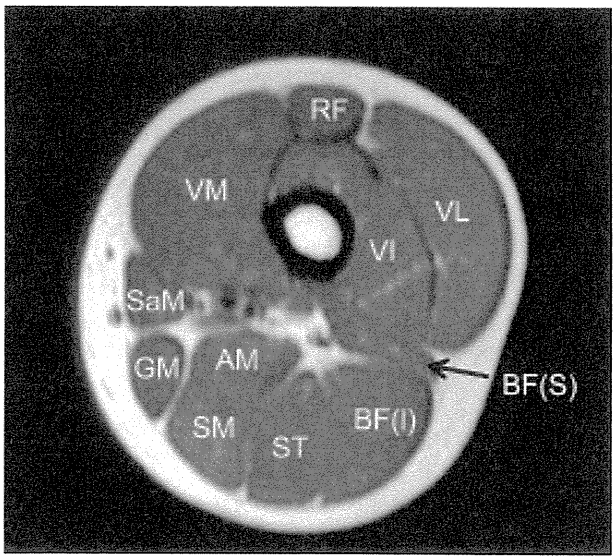

Fig. 2. Cross sectional area of thigh muscles.
The semitendinous muscles which were to be collected for subsequent DNA microarray analyses were measured in an MRI. VL, vastus lateralis; VM, vastus medialis; VI, vastus intermedius; RF, rectus femoris; BFL, biceps femoris long head; BFS, biceps femoris short head; ST, semitendinous muscle; SM, semimembranosus muscle; AM, Adductor muscles, SaM, Sartorius muscle; GM, Gracilis muscle.

Sampling of human skeletal muscle and RNA isolation

All patients in this study underwent ACL reconstruction surgery after training with hybrid exercise, electrical stimulation alone, or without electrical stimulation, as described above. In the ACL reconstruction surgery, the semitendinosus tendon must be prepared as a self-graft. After obtaining informed consent from all patients, a small amount of muscle attached to this tendon, which was redundant for the graft, was collected for the present study. The samples were immediately frozen in liquid nitrogen and stored at −80°C until the analyses.

Total RNA was isolated from the semitendinosus-muscles using RNA isolation solution (Nippon Gene, Tokyo, Japan) according to the manufacturer's instructions. The RNA pellets were resuspended in diethyl pyrocarbonate1-treated water. The quantity and quality of RNA obtained were estimated by an Agilent 2100 Bioanalyzer (Agilent Technologies, Santa Clara, CA, USA).

DNA microarray analysis

Isolated total RNA was analyzed by DNA microarray analysis using the human genome U133 set (Affymetrix, Santa Clara, CA, USA), which includes-33,000 human genes, according to the standard protocol recommended by Affymetrix (http://www.affymetrix.com/support/technical/manual/expression manual.affx) [10]. Gene intensity information was converted to a mean intensity for each gene by a proprietary software, Suite ver. 4.0 (Affymetrix), which includes routines for filtering and normalization. The intensity information was then transferred to an Excel software program (Microsoft Japan, Tokyo, Japan) and analyzed as needed.

Gene ontology analysis

A Gene Ontology (GO) database (as of September 18, 2009) was downloaded from the Gene Ontology website (http://www.geneontology.org/). GO analysis was performed with a software package, GeneSpring

ver. 8.0 (Agilent Technologies Santa Clara, CA, USA) [11]. GO analysis identified affected genes and created an "Entity List" on the basis of information gained in the array analysis. GO analysis further calculated the probability of matching between the database and the "Entity List". Probability values less than 0.05 were considered to indicate statistical significance.

Real-time reverse transcription and polymerase chain reaction

To confirm the expression of representative genes, we performed real-time reverse transcription and polymerase chain reaction (RT-PCR) analysis with the appropriate primers (Table 1) and SYBR Green dye using a real-time PCR system (model ABI 7300; Applied Biosystems, Foster City, CA, USA) according to the manufacturer's instructions [12]. Briefly, first-strand cDNAs were reverse transcribed at 42°C for 60 min and 95°C for 5 min from 1 μg of the extracted total RNA with Moloney murine leukemia virus reverse transcriptase (Promega, Madison, WI, USA) and primers (oligo-dT15 primer:random nonamer=1:10). The reaction mixture containing reverse-transcribed cDNAs was preheated for 2 min at 50°C and for 10 min at 95°C to activate *Taq* polymerase. A 40-cycle two-step PCR was performed, consisting of 15 sec at 95°C and 1 min at 60°C. The amount of target mRNA was calculated in the linear phase and normalized using glyceraldehyde-3-phosphate dehydrogenase (GAPDH) as an internal standard according to the delta-delta Ct method [13].

RESULTS

Cross sectional area of semitendinosus muscle in the affected limb

Table 2 shows the CSA of the semitendinosus muscles in the affected limb before and after the exercise period. After the exercise, CSA had increased in size by 4.2 and 14.7%, respectively, in the two hybrid exercise subjects, and by 1.4% in the subject with electrical stimulation. However, it had shrunk by 7.7% in the subject without electrical stimulation. One hybrid exercise subject, a 16-year-old male, started the

TABLE 1.
Primers for the polymerase chain reaction

Target gene	Sequence	Length (bp)
EIF5A	S:5'-CACCCCACAGAGCAAGTTTT-3'	148
	AS:5'-AGCACCACAAAGCCATTCTT-3'	
PEX6	S:5'-CAGAATTCAGAGGTACTTGGAAGG -3'	176
	AS:5'-CCCTGGGTATCTGAAAGTGC-3'	
FHOD3	S:5'-GTCTGAGCTATGCGGAGGAC-3'	170
	AS:5'- ATTGGGCGAGTCATCAGTTC-3'	
GAPDH	S: 5'-ACCCAGAAGACTGTGGATGG-3'	125
	AS: 5'-TTCAGCTCAGGGATGACCTT-3'	

AS, antisense primer; S, sense primer; EIF5A, eukaryotic translation initiation factor 5A; PEX6, peroxisomal biogenesis factor 6; FHOD3, formin homology 2 domain containing 3; GAPDH, glyceraldehyde-3-phosphate dehydrogenase.

TABLE 2.
Profile of subjects and cross-sectional area (CSA) of semitendinosus muscles in the affected limb before and after exercise period

exercise	age gender	after injury (weeks)	CSA of semitendinous muscle		
			before (mm^2)	after (mm^2)	after/before ratio (%)
hybrid	16 yrs old male	24	901	940	104.2
	24 yrs old male	12	633	726	114.7
electrical stimulation	16 yrs old male	16	780	790	101.4
without electrical stimulation	15 yrs old female	8	372	343	92.3

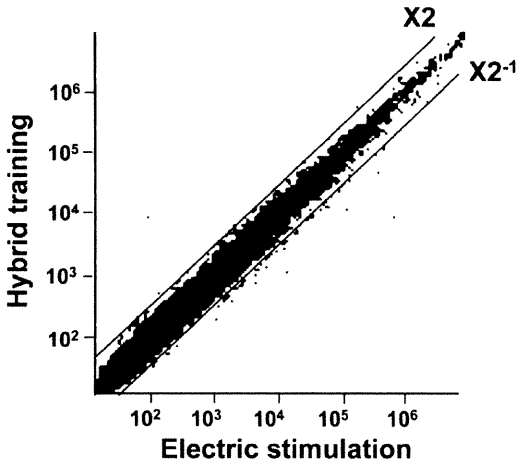

Fig. 3. Gene expression in the semitendinosus muscle.

The gene expression in hybrid exercise was compared with that in electrical stimulation. Genes with a similar expression lie on a line from the origin to the top right corner; the expression level is indicated by the distance from the origin. The scale on each axis is log scale.

exercise 24 weeks after injury. CSA was 901 mm^2 before the exercise and 940 mm^2 after the exercise. The ratio of CSA after/before exercise was 104.2%. The other hybrid exercise subject, a 24-year-old male, started the exercise 12 weeks after injury. CSA was 633 mm^2 before the exercise and 726 mm^2 after the exercise. The ratio of CSA after/before exercise was 114.7%. The subject with electrical stimulation, a 16-year-old male, started the exercise 16 weeks after injury. CSA was 780 mm^2 before the exercise and 790 mm^2 after the exercise. The ratio of CSA after/before exercise was 101.4%. The subject without electrical stimulation, a 15-year-old female, started the exercise 8 weeks after injury. CSA was 372 mm^2 before the exercise and 343 mm^2 after the exercise. The ratio of CSA after/before exercise was 92.3%.

Comprehensive gene expression and GO analyses

The samples were analyzed with a microarray, and a scatter plot was generated (Fig. 3). Genes with an absolute value of less than 500 were excluded. Genes that exhibited increased or decreased levels of expres-

TABLE 3.
Functional classification of 125 genes (Up, top 75 genes; Down, top 50 genes) that exhibited increased or decreased expression levels after hybrid exercise in comparison to electrical stimulation

	Up	Down
Membrane receptor	1	0
Transporter and channel	3	1
Gene expression control		
Signal transduction	14	3
Transcription-related	10	9
Translation-related	2	2
Adhesion and membrane protein	2	2
Cell structure, including cytokinesis, sorting, fusion, and motor protein and motor protein	8	1
Growth factor, secreted protein, and matrix protein and motor protein	1	0
Metabolism	4	4
Mitochondrial protein and gene	2	1
Cell cycle	1	3
Heat shock protein and chaperonin	0	0
Stress response gene	1	0
Heat shock protein and chaperonin	0	0
Ubiquitin-proteasome-related gene	5	4
Other protease-related gene	2	0
Apoptosis	0	1
EST and others	19	19
total	75	50

The sequences of expression sequence tag (EST) genes were subjected to the BLAST retrieval system to search for similar genes.

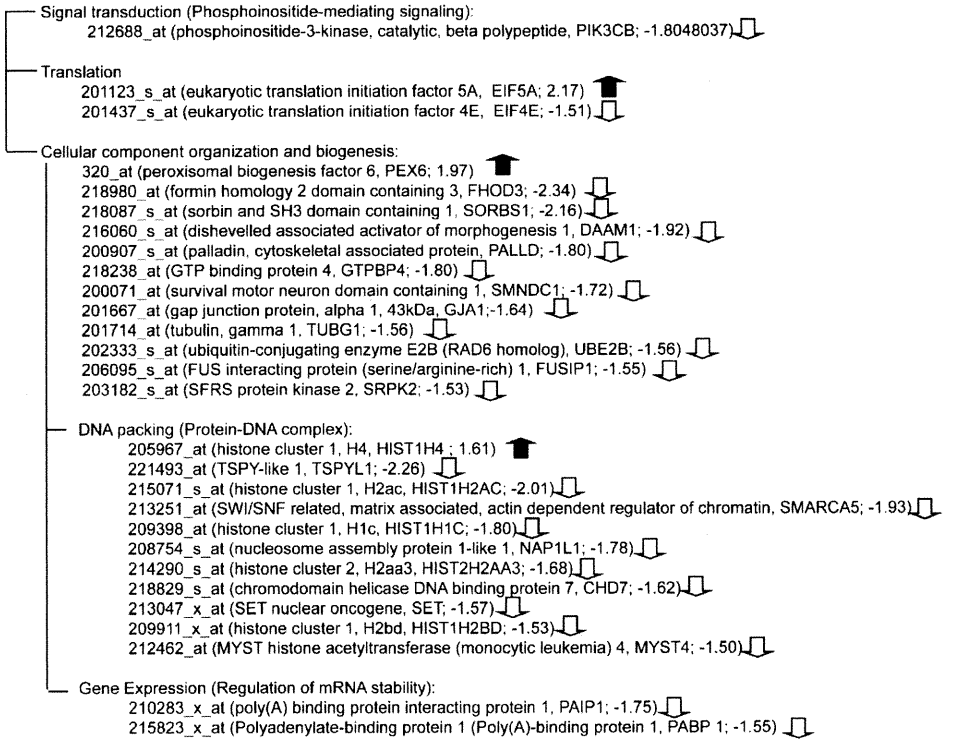

Fig. 4. GO analysis.

GO analysis was performed with a software package, GeneSpring ver. 8.0 (Agilent Technologies). GO analysis classified genes on microarray chips to potent affected genes as "Entity List" on the basis of information gained array analysis. GO analysis further calculates the probability of matching the accurate probability test (direct probability) from the list of categorized "Entity List". Probability values less than 0.05 were considered to be statistically significant.

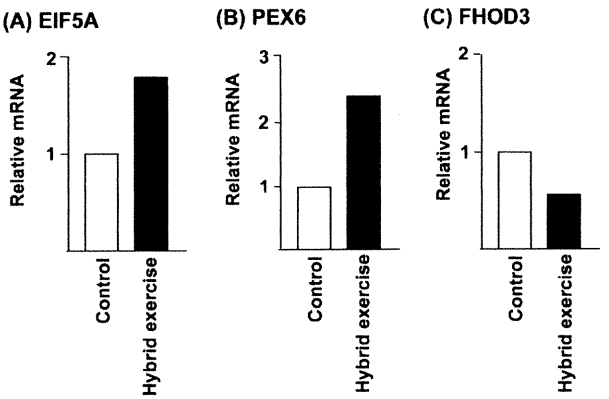

Fig. 5. Expression of EIF5A, PEX6 and FHOD3 in semitendinosus muscles.

Expression of EIF5A (A), PEX6 (B) and FHOD3 (C) transcripts in semitendinosus muscles was assessed by real-time RT-PCR analysis. The fluorescence ratio of the target gene cDNA to GAPDH, a house keeping gene, was calculated. Data are shown as the mean in the hybrid exercise group (n=2), compared with the mean in the control 1 (electrical stimulation, n=1) and control 2 (without electrical stimulation, n=1) groups.

sion were chosen and their functions were classified (Table 3). The results showed that hybrid exercise preferentially promoted the expression of genes associated with signal transduction (14 genes) transcription (10 genes) and cell structure (7 cytoskeletal genes, and 1 sorting gene).

Because the number of candidates for the experiments was limited, we were unable to obtain a sufficient number of skeletal muscles for statistical analysis during this experiment period. Therefore, we performed GO analysis to classify the genes that were significantly changed by hybrid exercise. The GO analysis revealed that hybrid exercise induced significantly higher expression levels of several genes, i.e. eukaryotic translation initiation factor 5A (EIF5A), peroxisomal biogenesis factor 6 (PEX6), and histone cluster 1 H4 (HIST1H4), compared with electrical stimulation alone (Fig. 4). In contrast, the expression of various genes associated with signal transduction, translation, and cellular component organization and biogenesis was suppressed by hybrid exercise (Fig. 4).

We also confirmed the effect of hybrid exercise on the expression of some of these genes by real-time RT-PCR (Fig. 5).

DISCUSSION

"Hybrid exercise" is an exercise method that combines electrically stimulated and volitional contraction. When the joint is volitionally flexed, the extensor muscle is electrically stimulated, and when the joint is volitionally extended, the flexor muscle is electrically stimulated. Therefore, hybrid exercise achieves adequate loading of muscles during both extensor and flexor movements.

In ACL reconstruction surgery, the semitendinosus tendon is prepared as a self-graft. A small amount of muscle attached to this tendon, which was redundant for the graft, was collected during the operation. Hybrid exercise was performed with these preoperative ACL-injured patients, and the muscle tissue which would have been abandoned was used in the experiment. This was why we used ACL-injured patients as the subjects for this study. However we were unable to obtain a sufficient number of skeletal muscles for statistical analysis during the experimental period because the number of candidates was limited.

Preoperative quadriceps strength is considered a significant predictor of knee function after ACL reconstruction surgery [14], and quadriceps exercise has been widely performed before reconstruction surgery. The current study was carried out to evaluate the mechanism of the effect of hybrid exercise and not to show its efficacy in ACL-injured patients. To prove the clinical efficacy of hybrid exercise in ACL-injured patients, a large clinical trial will be required in future.

To elucidate the mechanism of the apparent beneficial effect of hybrid exercise, we examined the comprehensive gene expression profiles in muscles trained by hybrid exercise and compared them with the profiles in control muscles subjected to electrical stimulation alone or without electrical stimulation. The microarray analysis showed that hybrid exercise preferentially promoted the expression of genes associated with signal transduction and transcription, and cytoskeletal genes, as compared with electrical stimulation alone. Our results suggest that hybrid exercise helps to maintain muscle mass after unloading, possibly through this distinct gene expression pattern, although additional studies with larger patient groups will be needed to substantiate this hypothesis.

This is the first report to address the relationship between gene expression and the effect of hybrid exercise. Future GO analyses based on the microarray information obtained herein may further clarify the mechanisms of the beneficial effects of hybrid exercise. The present GO analysis revealed that hybrid exercise induced significantly higher expression of EIF5A and PEX6, compared with electrical stimulation alone, while expression of a variety of genes was suppressed by hybrid exercise. EFA5A is a translation initiation factor, and has previously been shown to have a strong association with the protein synthesis process [15]. Muscle protein synthesis plays a central role in the recovery from muscle atrophy or aging. In fact, the reduction of the EFA5A level in the cerebellum contributes to the impairment of long-term motor memory that is observed during aging [16]. Furthermore, EIA5A enhances muscle regeneration through its role in satellite cell (skeletal muscle stem cell) differentiation [17]. In contrast, peroxisome biogenesis, for which PEX6 is a prerequisite factor [18], plays an important role in muscle regeneration after injury [19].

On the basis of these findings, we suggest that hybrid exercise may stimulate muscle regeneration, perhaps through enhanced expression of EIF5A and PEX6, and may thereby contribute to muscle strengthening. Further studies will be needed to confirm this hypothesis.

ACKNOWLEDGMENTS: We would like to thank Takashi Maeda PT for his valuable assistance in the hybrid exercise. We also thank Yoshio Takano PT for CSA measurement. This study was carried out as part of the "Ground-based Research Announcement for Space Utilization" promoted by the Japan Space Forum.

REFERENCES

1. Matsuse H, Shiba N, Umezu Y, Nago T, Tagawa Y et al. Muscle training by means of combined electrical stimulation and volitional contraction. Aviat Space Environ Med 2006; 77:581-585.
2. Iwasaki T, Shiba N, Matsuse H, Nago T, Umezu Y et al. Improvement in knee extension strength through training by means of combined electrical stimulation and voluntary muscle contraction. Tohoku J Exp Med 2006; 209:33-40.
3. Takano Y, Haneda Y, Maeda T, Sakai Y, Matsuse H et al. Increasing Muscle Strength and Mass of Thigh in Elderly People with the Hybrid-Training Method of Electrical Stimulation and Volitional Contraction. Tohoku J Exp Med 2010; 221:77-85.
4. Yanagi T, Shiba N, Maeda T, Iwasa K, Umezu Y et al. Agonist contractions against electrically stimulated antagonists. Arch Phys Med Rehabil 2003; 84:843-848.
5. Jagoe RT, and Goldberg AL. What do we really know about the ubiquitin-proteasome pathway in muscle atrophy? Curr Opin Clin Nutr Metab Care 2001; 4:183-190.

6. Rommel C, Bodine SC, Clarke BA, Rossman R, Nunez L et al. Mediation of IGF-1-induced skeletal myotube hypertrophy by PI(3)K/Akt/mTOR and PI(3)K/Akt/GSK3 pathways. Nat Cell Biol 2001; 3:1009-1013.
7. Bodine SC, Stitt TN, Gonzalez M, Kline WO, Stover GL et al. Akt/mTOR pathway is a crucial regulator of skeletal muscle hypertrophy and can prevent muscle atrophy in vivo. Nat Cell Biol 2001; 3:1014-1019.
8. Ogino M, Shiba N, Nagata K, Iwasa K, Tagawa Y et al. MRI quantification of muscle activity after volitional exercise and neuromuscular electrical stimulation. Am J Phys Med Rehabil 2002; 81:446-451.
9. Ward AR, and Shkuratova N. Russian electrical stimulation: the early experiments. Phys Ther 2002; 82:1019-1030.
10. Nikawa T, Ishidoh K, Hirasaka K, Ishihara I, Ikemoto M et al. Skeletal muscle gene expression in space-flown rats. FASEB J 2004; 18:522-524.
11. Nelson GM, Ahlborn GJ, Delker DA, Kitchin KT, O'Brien TG et al. Folate deficiency enhances arsenic effects on expression of genes involved in epidermal differentiation in transgenic K6/ODC mouse skin. Toxicology 2007; 241:134-145.
12. Ogawa T, Nikawa T, Furochi H, Kosyoji M, Hirasaka K et al. Osteoactivin upregulates expression of MMP-3 and MMP-9 in fibroblasts infiltrated into denervated skeletal muscle in mice. Am J Physiol Cell Physiol 2005; 289:C697-707.
13. Livak JK, and Schmittgen TD. Analysis of relative gene expression data using real-time quantitative PCR and the 2(-Delta Delta C(T)) Method. Methods 2001; 25:402-408.
14. Eizen I, Holm I, and Rsiberg MA. Preoperative quadriceps strength is a significant predictor of knee function two years after anterior cruciate ligament reconstruction. Br J Sports Med 2009; 43:371-376.
15. Kang HA, and Hershey JW. Effect of initiation factor eIF-5A depletion on protein synthesis and proliferation of Saccharomyces cecervisiae. J Biol Chem 1994; 269:3934-3940.
16. Luchessi AD, Cambiaghi TD, Alves AS, Parreiras-E-Silva LT, Britto LR et al. Insights on eukaryotic translation initiation factor 5A (eIF5A) in the brain and aging. Brain Res 2008; 4:1228:6-13.
17. Luchesi AD, Cambiaghi TD, Hirabara SM, Lambertucci RH, Silveira LR et al. Involvement of eukaryotic translation initiation factor 5A (eIF5A) in skeletal muscle stem cell differentiation. J Cell Physiol 2009; 218:480-489.
18. Fujiki Y, Miyata N, Matsumoto N, and Tamura S. Dynamic and functional assembly of the AAA peroxins, Pex1p and Pex6p, and their membrane receptor Pex26p involved in shuttling of the PTS1 receptor Pex5p in peroxisome biogenesis. Biochem Soc Trans 2008; 36:109-113.
19. Matsuura T, Li Y, Giacobino JP, Fu FH, and Huard J. Skeletal muscle fiber type conversion during the repair of mouse soleus: potential implications for muscle healing after injury. J Orthop Res 2007; 25:1534-1540.

Mitsui et al. BMC Musculoskeletal Disorders 2011, 12:18
http://www.biomedcentral.com/1471-2474/12/18

BMC Musculoskeletal Disorders

RESEARCH ARTICLE Open Access

Hyperadiponectinemia enhances bone formation in mice

Yasuhiro Mitsui[1], Masafumi Gotoh[2*], Nobuhiro Fukushima[1], Isao shirachi[1], Shuichi Otabe[3], Xiaohong Yuan[3], Toshihiko Hashinaga[3], Nobuhiko Wada[3], Akiko Mitsui[3], Tatsuhiro Yoshida[1], Shiro Yoshida[2], Kentaro Yamada[3], Kensei Nagata[1]

Abstract

Background: There is growing evidence that adiponectin, a physiologically active polypeptide secreted by adipocytes, controls not only adipose tissue but also bone metabolism. However, a role for adiponectin in bone development remains controversial.

Methods: We therefore investigated the endocrine effects of adiponectin on bone metabolism using 12-week-old male transgenic (Ad-Tg) mice with significant hyperadiponectinemia overexpressing human full-length adiponectin in the liver.

Results: In Ad-Tg mice, the serum level of osteocalcin was significantly increased, but the levels of RANKL, osteoprotegerin, and TRAP5b were not. Bone mass was significantly greater in Ad-Tg mice with increased bone formation. In contrast, bone resorption parameters including the number of osteoclasts and eroded surface area did not differ between Ad-Tg and their littermates.

Conclusions: These findings demonstrate that hyperadiponectinemia enhances bone formation in mice.

Background

Osteoporosis and related bone fractures are becoming increasingly common in industrial countries due to enhanced longevity [1,2]. Therefore, it is important to know the factors that regulate bone mass, and to develop effective therapeutic methods.

Adipose tissue is known to act as an energy-storing organ that secretes a variety of biologically active molecules [3]. Adiponectin is one of the adipocytokines specifically and highly expressed in adipose tissue. It has two subtypes: the full-length (predominant) form that is distributed in the circulation, and the globular form [4]. This adipocytokine is present abundantly in plasma [5] and plays important roles in the regulation of energy homeostasis and insulin sensitivity [6,7], thus exerting potent effects in various tissues.

It has been reported that the adiponectin signal is also involved in bone homeostasis, since adiponectin and its two related adiponectin receptor subtypes (AdipoR1 and AdipoR2) have been identified in osteoblasts [8-10]. Although previous studies have examined the effect of adiponectin on bone metabolisms, its physiological role remains unclear [9-13].

Recently, we have successfully established two lines of hyperadiponectinemic mice showing transgenic expression of human full-length adiponectin [14]. To test the hypothesis that the level of circulating human full-length adiponectin is positively correlated with bone metabolism, the present study focused on characterizing its endocrine effect in this strain of transgenic mice. We demonstrated that hyperadiponectinemia enhances osteogenesis through osteoblast formation.

Methods

Animals

Transgenic (Ad-Tg) mice overexpressing human full-length adiponectin, driven by the human serum amyloid component (SAP) promoter and with its expression limited to the liver, were generated as described previously [14]. In each analysis, male Ad-Tg and their wild

* Correspondence: gomasa@med.kurume-u.ac.jp
[2]Department of Orthopedic Surgery, Kurume University Medical Center, 155 Kokubu-machi, Kurume, Fukuoka 839-0863, Japan
Full list of author information is available at the end of the article

type (WT) littermates generated by intercrossing between heterozygous mice were compared. All the mice were kept in plastic cages under standard laboratory conditions with a 12-h dark, 12-h light cycle, a constant temperature of 23°C, and a humidity of 48%. The mice were fed a standard rodent diet (CE-2; CLEA Japan, Inc.) containing 25.2% protein, 4.6% fat, 4.4% fiber, 6.5% ash, 3.44 Kcal/g, 2.5 IU vitamin D_3/g, 1.09% calcium, and 0.93% phosphorus with water ad libitum. All animal experiments were performed on male mice at 12 weeks of age and were reviewed and approved by the Animal Study Committee of Kurume University.

Skeletal morphology

There were 8 mice in each group (Lines 11 and 13 representing Ad-Tg mice, and their WT littermates): the right femur was used for bone mineral density (BMD) and bone mineral content (BMC) analysis, and the left tibia for bone histomorphometric evaluation. A total of 24 mice were sacrificed and analyzed in this study. BMD and BMC were measured in 24 femurs (8 femurs in each mouse group) using a DCS-600EX-IIIR (Aloka). Twenty-four tibiae (8 tibiae in each mouse group) were fixed in 70% ethanol, and the undecalcified bones were embedded in glycolmethacrylate. Sections 3 μm thick were cut longitudinally in the proximal region of the tibiae, and stained with toluidine blue. Histomorphometry was performed with a semiautomatic image analysis system (Histometry RT CAMERA, System Supply) linked to a light microscope. The histomorphometric measurements were made at ×400 using a minimum of 27-37 optical fields in the secondary spongiosa area at the growth plate-metaphyseal junction. The bone was labeled with calcein twice, with a 4-day interval between. The bone formation rate and mineral apposition rate were measured at the proximal tibia after calcein injection (16 mg/kg, Dojin). Nomenclature, symbols, and units are those recommended by the Nomenclature Committee of the American Society for Bone and Mineral Research [15].

Blood chemistry

Blood was taken just before death, and the serum was prepared. The level of human and mouse adiponectin was measured using an ELISA kit for the human form (Otsuka) and mouse form (AdipoGen). Mouse insulin and leptin were determined using ELISA kits (Genzyme). Serum levels of RANKL, osteocalcin (OC), OPG and TRAP5b in serum were determined by ELISA with a mouse osteocalcin EIA kit (Biomedical Technologies), a mouse TRAP5b ELISA kit (Immunodiagnostic Systems), a mouse RANKL immunoassay kit (R&D Systems), and a mouse OPG immunoassay kit (R&D Systems), respectively. Assays were performed in accordance with the manufacturer's recommendation.

Statistical analysis

All data are presented as mean ± S.D., and statistical analysis was performed by ANOVA with Dunnett adjustment. Differences were considered statistically significant at $P < 0.05$.

Results

Transgenic (Ad-Tg) mice overexpressing human full-length adiponectin in the liver

To examine the endocrine effect of human adiponectin on bone metabolism, we analyzed two lines of 12-week-old male Ad-Tg mice overexpressing human adiponectin mRNA exclusively in the liver [14]. There was no human adiponectin expression in other tissue: muscle, visceral fat, spleen, or brain. The liver was histologically normal, with levels of hepatic enzymes similar to those in their WT littermates [14]. Ad-Tg mice in each line grew normally, were fertile, and appeared healthy with no gross histomorphological abnormalities. Measurement of the serum level of human and mouse full-length adiponectin in Ad-Tg mice using human and mouse adiponectin-specific ELISA demonstrated significant hyperadiponectinemia (Figure 1A, B). The plasma level was elevated in human adiponectin Tg mice, indicating a lack of negative feedback regulation. This finding had also been noted in our previous study [14]. Although the precise mechanisms responsible for the increase of endogenous mouse adiponectin in human adiponectin Tg mice was not clarified in the present study, it is conceivable that transgenic expression of adiponectin results in an increase in the total level of circulating adiponectin. The serum levels of leptin and insulin did not differ significantly between Ad-Tg mice and their WT littermates [14]. Thus, the Ad-Tg mice used in the present study were considered to be an appropriate model for characterizing the endocrine effect of human full-length adiponectin on bone metabolism.

Serum levels of osteoblastic and osteoclastic markers

Firstly, we evaluated the levels of osteoblastic and osteoclastic markers in the serum of Ad-Tg and WT mice (Table 1). The serum osteocalcin (OC) level has long been used as a marker of osteoblast activity and new bone formation [16,17]. We therefore measured the level of OC in serum using a specific mouse OC ELISA to evaluate osteoblast activity in WT and Ad-Tg mice. The results showed that the serum OC level was significantly higher in the Ad-Tg mice than in their WT littermates, suggesting that osteoblastgenesis is increased in Ad-Tg mice. To evaluate osteoclast activity, the serum level of active TRAP5b, an enzyme that is released from osteoclasts during bone resorption [18], was examined and compared between Ad-Tg and WT

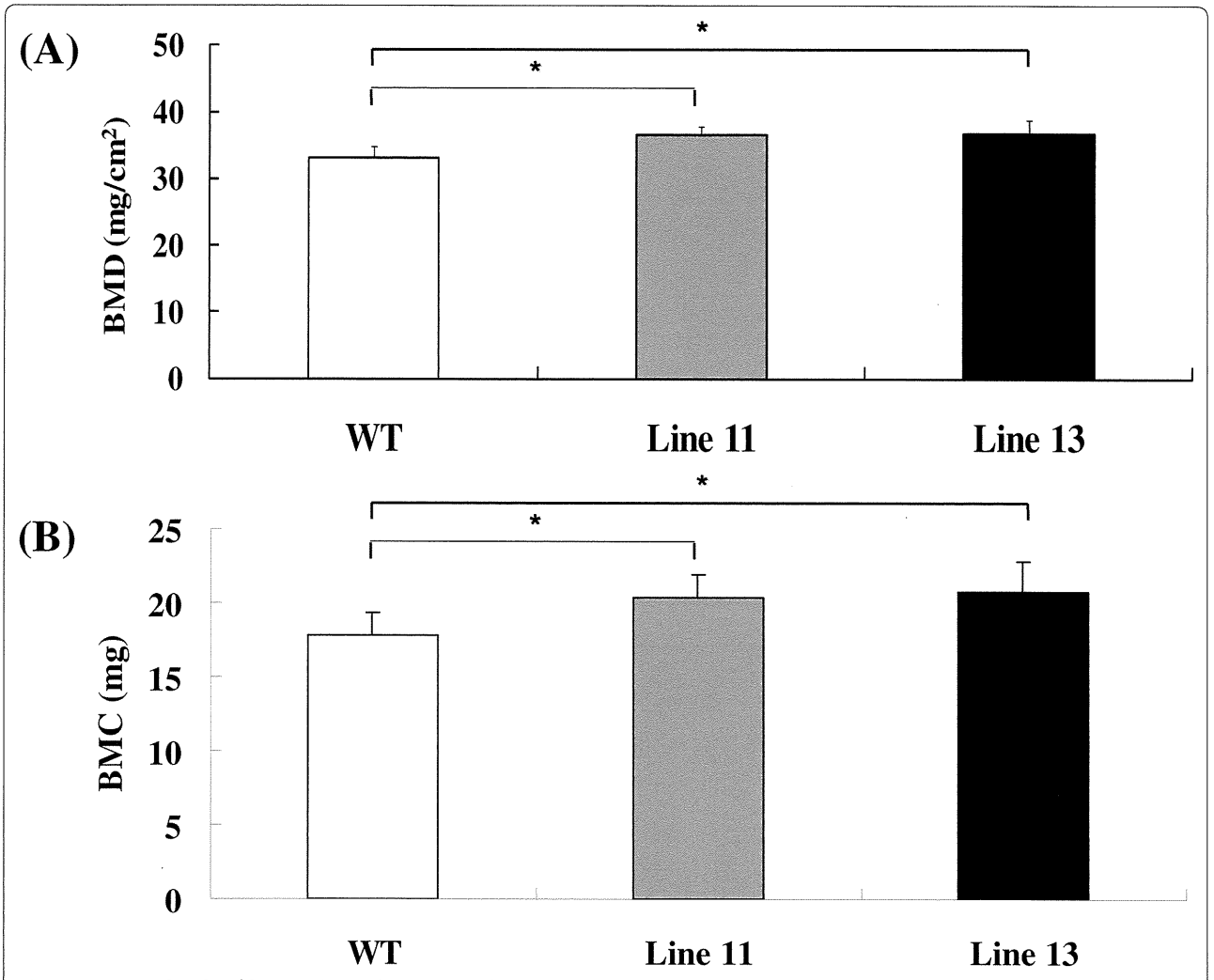

Figure 1 Serum levels of human (A) and mouse (B) full-length adiponectin in 12-week-old Ad-Tg and WT littermate mice. Data are expressed as means (bars) ± S.D. (error bar), n = 8. ND, not detected. Significant difference from WT serum level, $P < 0.05$.

mice. Unlike the serum OC level, the serum TRAP5b level demonstrated no significant difference between Ad-Tg and WT mice. To substantiate this further, we next measured the serum levels of RANKL and OPG, which are essential factors for osteoclast formation [19,20]. In accord with the results for TRAP5b, the serum levels of RANKL and OPG showed no significant difference between Ad-Tg and Wt mice.

Table 1 Serum levels of osteocalcin, TRAP5b, RANKL and OPG in 12-week-old Ad-Tg and WT littermate mice

	WT	Ad-Tg Line11	Ad-Tg Line13
Osteocaltin (ng/ml)	25.2 ± 1.1	27.8 ± 0.8**	27.7 ± 0.9**
TRAP5b (U/L)	2.2 ± 0.4	2.1 ± 0.3	2.3 ± 0.4
RANKL (pg/ml)	68.6 ± 7.2	82.0 ± 24.6	77.1 ± 29.1
OPG (ng/ml)	2226.9 ± 61.4	2251.5 ± 212.0	2521.9 ± 277.8

Data are expressed as means ± S.D. (n = 8). **Significant difference from WT serum level, $P < 0.05$.

Histomorphometric analysis of Ad-Tg mice

To examine the role of endogenous human full-length adiponectin in bone metabolism, we analyzed the long bones of Ad-Tg mice and WT littermates at 12 weeks of age. BMD and BMC of the whole femur were consistently higher in Ad-Tg than in WT mice (Figure 2A, B).

Bone histomorphometric analysis was performed at the proximal tibiae in Ad-Tg and WT mice (Table 2). Bone volume was significanty increased due to the presence of human full-length adiponectin. Osteoblast surface and osteoid surface, both representative of the number of osteoblasts, were significantly greater in Ad-Tg mice than in their WT littermates. In contrast, bone resorption parameters including osteoclast number and eroded surface area, did not differ between the two types of mice. The mineral apposition rate, which reflects the bone formation ability of individual osteoblasts, was significantly higher in Ad-Tg mice (Table 2).

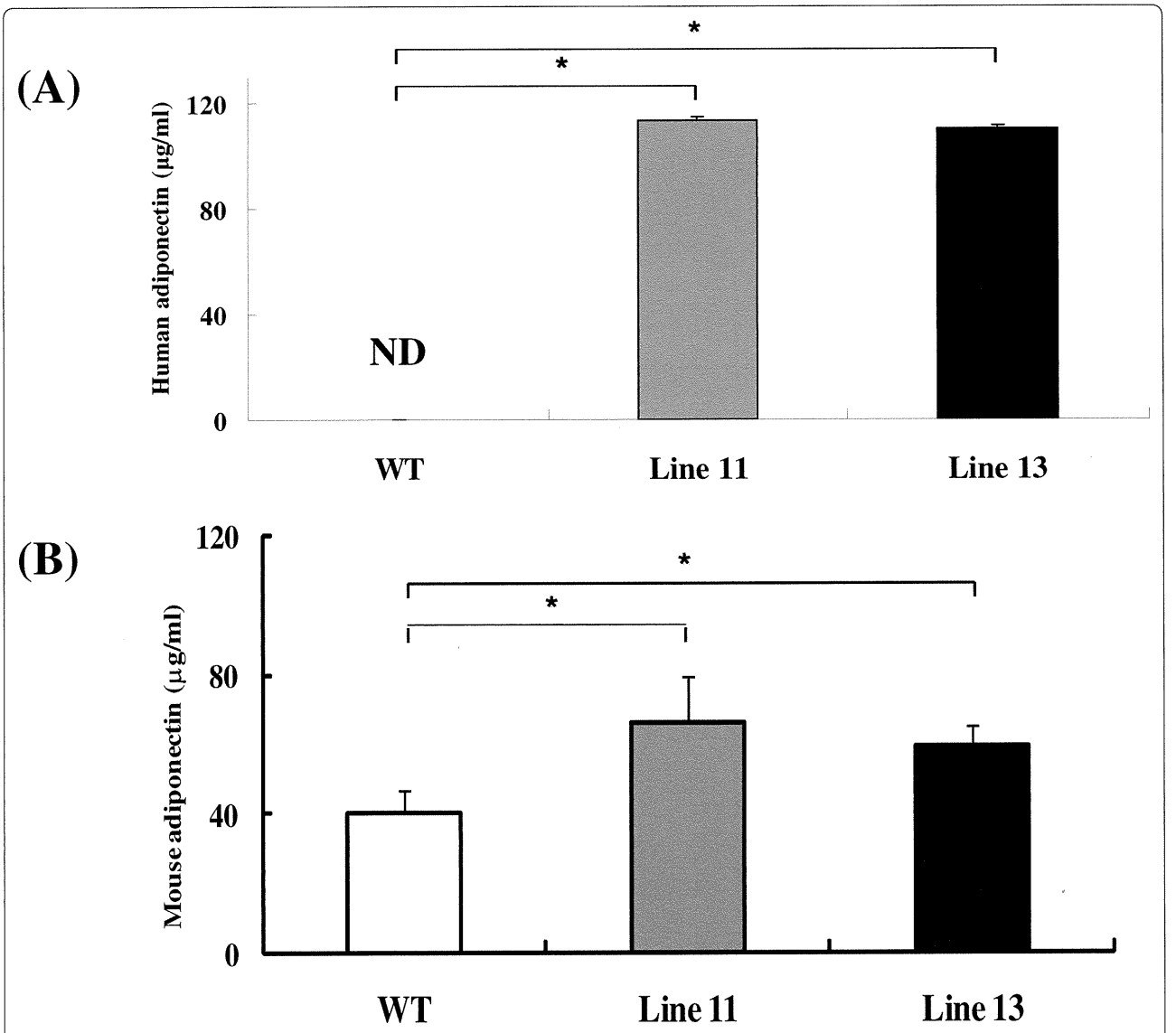

Figure 2 BMD (A) and BMC (B) of the entire femur were measured by DEXA. Data are expressed as means (bars) ± S.D. (error bar), n = 8. Significant difference from WT mice, $P < 0.05$.

Calcein double labeling showed that the width between the labeled sections in Ad-Tg mice was significantly increased than that in the WT littermates. Thus, Ad-Tg mice exhibited a high bone mass with increased bone formation but normal osteoclast function.

Discussion

A few studies using Ad-Tg mice have assessed the role of adiponectin in bone metabolism, but the results have been conflicting [8,10,21]. Oshima et al. demonstrated that transient overexpression of full-length mouse adiponectin for 2 week by adenoviral infection in 8-week-old C57BL/6J mice increased trabecular bone volume in the distal femur compared with LacZ overexpressing controls, with reduced number of osteoclasts in TRAP-stained sections [8]. These results concurred with our data in view of increased bone mass; however, they did not report the serum levels of adiponectin, insulin, and body weights. Shinoda *et al.* demonstrated no significant differences in bone mass or turnover in 8-week-old male Ad-Tg mice overexpressing globular-type adiponectin specifically in the liver, compared to their WT littermates [10]. In their study, no differences in BMD of the femur, tibia, and vertebrae and no differences in bone formation or resorption parameters were found in Ad-Tg mice [10]. Recent studies have demonstrated that the biological effect of adiponectin depends on its molecular structure [22,23], suggesting that the full effects of adiponectin on bone may be mediated by full-length adiponectin, rather than the globular type.